Asian Journal of Atmospheric Environment
Vol. 6-3, pp.234-243, September 2012
doi: http://dx.doi.org/10.5572/ajae.2012.6.3.234

High Loading for Air Pollution in the Byunsan Peninsula of Korea by an Interplay of the Saemangeum Project and Winter Monsoon

Chang-Jin Ma*, Gong-Unn Kang[1)] and Ki-Hyun Kim[2)]

Department of Environmental Science, Fukuoka Women's University, Fukuoka 813-8529, Japan
[1)]Department of Medical Administration, Wonkwang Health Science University, Iksan 570-750, Korea
[2)]Department of Environment & Energy, Sejong University, Seoul 143-747, Korea

*Corresponding author. Tel: +81-92-661-2411, Fax: +81-92-661-2415, E-mail: ma@fwu.ac.jp

ABSTRACT

The wintertime high loading for atmospheric pollutants is certainly expected in the Byunsan Peninsula of Korea because of a great-scale reclamation project having construction of 33 km tidal sea dike impounding an area of over 40,000 ha and long-range transport. The goal of this study is to trace the origin of this wintertime burden for ambient particulate matter (hereafter called "PM") in the Byunsan Peninsula of Korea. The size-segregated (i.e., cutoff size from 0.01 μm to 4.7 μm) PM sampling was conducted at a ground-based site of Byunsan Peninsula located in the west coast of Korean Peninsula during the height of dike constructing. Data archived in this study are the mass concentrations of ionic, elemental, and carbonic components in size-fractioned PM. The elemental mass of individual submicrometer particles was also analyzed. The sum of 5-source (i.e., elemental carbon, organic materials, inorganic secondary pollutants, crustal matter, and sea-salts) concentrations shows the bimodal distribution (major and minor peaks formed around D_p, 0.65 μm and D_p, 4.7 μm, respectively) by border with 0.19 μm of cutoff size. The concentrations of EC in $PM_{1.1\text{-}0.01}$ in winter and spring times were 4.62 μg m^{-3} and 3.74 μg m^{-3}, respectively. Elemental masses of submicron individual particles are classified into two groups, i.e., the major elements (Cl, Al, Si, S, and P) and the minor trace elements. Cluster analysis differentiated the elements in submicron individual particles into 4-cluster. Among them, three clusters are in agreement with the major (Al, Si, S, and P), minor (Fe, Ca, and K), and trace compositions of coal burning. Meanwhile, Cl classified as an independent cluster has different source profile which was mainly due to the Saemangeum seawall project. Some highly toxic elements (e.g., Cr, Mn, and As (and/or Pb)) were also detected in some part of submicron individual PM. As a consequence, the combination of the Saemangeum project and winter monsoon played a considerable part in the double aggravation of wintertime air pollution in the Byunsan Peninsular.

Key words: Saemangeum project, Wintertime atmosphere, Byunsan Peninsula, Elements, Long-range transport

1. INTRODUCTION

The Saemangeum lay at the mouths of the Dongjin and Mangyeong Rivers, on central west coast of South Korea. It was dammed by the government of South Korea's Saemangeum Seawall Project, completed in April 2006. The Saemangeum development project is a national project to build a global city as a frontrunner of green growth. The project created the world's longest man-made dike, measuring 33 kilometers and 400 square kilometers of farmland and a freshwater reservoir.

Mobilized equipments (including heavy dump trucks and dredging equipments) and people to construct the Saemangeum dike were up to 910,000 and 2,370,000 per year, respectively. The total amount of soil and stone that were dumped into sea was 123,000,000 m^3 (Jajuminbo, 2010).

The pollutants in China are one of major concerns in Korea, particularly in the western parts of peninsular that are located too close to Chinese continent because pollutants frequently pass over Yellow Sea through nearly a whole year and have been getting worse in resent year (Jhun and Lee, 2004; Wang *et al*., 2000).

When the air close to the earth is cooler than the air above it (i.e., a temperature inversion), the pollution cannot rise and disperse. Winter inversion will likely to lead to the air being more polluted than other seasons. The highest levels of pollutants in Korea during

wintertime are caused by both significant levels of home grown air pollutants and wintertime weather condition. Moreover, when the wind is blowing in from China this seasonal phenomenon can be altered for the worse (Kim, 2000). The inflow of pollutants from China continent into Korea Peninsula is outstanding in wintertime because Jets are especially stronger by the largest temperature gradients in winter. This inflow pollutant mixes with the local air pollution and causes not only low visibility, but also severe respiratory problems in the general population (McDonnell *et al*., 2000; Pope *et al*., 1999; Gulyas and Gercken, 1988). However, there remain a lot of uncertainties regarding the linkage between the locally emitted pollutants and the influence of Chinese continent, especially, under the wintertime meteological condition.

The main purpose of this study is to determine the chemical properties of wintertime particles collected in the Byunsan Peninsula of Korea which was subject to high loading of air pollutants under double influence of the Saemangeum seawall project and winter monsoon.

2. EXPERIMENTAL METHODS

2.1 Sampling of Size-fractionated Particles

A measurement of size-classified PM was made at Byunsan Peninsula, which is situated in the western part of Jeollabuk-do, Korea. Byunsan Peninsula leads to the West Sea (Yellow Sea) and is located very near the Chinese continent. For the sampling of aerosols as a function of their size (8-step classification between 0.43 μm and 11 μm), an Andersen air sampler (Tokyo Dylec Co., AN-200) was operated at the ground based site (35.37°N; 126.27°E, 30 meters above the sea), indicated by a filled circle in Fig. 1, during the winter (16-19 December) of 2003. This sampling site is located at southeast of the scene of dike construction. The time of our field measurement was just the peak of the dike constructing. The project was in full swing in December of 2003 and the construction of seawall connecting was finally completed on December 30, 2003.

For the purpose of getting comparative data, an additional field measurement was also carried out in spring (25-28 May) of 2004. In order to estimate ionic, elemental, and carbonaceous components as a function of particle size, multi kinds of filter media were arranged on each stage of sampler (i.e., a 25 mm diameter quartz fiber filter (Whatman) pretreated by heating in an electric furnace at 600°C for 3 h for carbon analysis, a 25 mm diameter Nucleporefilter® for single particle analysis, and a 47 mm diameter Nucleporefilter® for ion analysis). Sampling duration time was adjusted for 4 h and 72 h for single and bulk particle analyses, respectively.

During wintertime sampling period, the range of wind speed was 0.4-9.4 m s^{-1} and it was generally blowing from the northwest. The temperature and relative humidity were around −2.3-8.0°C and 53-61%, respectively.

After sampling, the filters were placed in clean sterilized petridishes. And then each petridish was sealed with Teflon tape and wrapped with aluminum foil and was placed in a cold storage bag during air transportation. Blank filters were handled in the same manner as the samples.

2.2 Bulk Analysis for Ionic and Carbonic Components

For the analysis of ionic species, filters were extracted with deionized water by ultrasonic treatment. Ion Chromatography (IC) (Dionex DX-100) was used to determine the concentrations of various ions present in the size-resolved particles. Samples were analyzed for both cations (sodium, ammonium, potassium, magnesium, and calcium) and anions (fluoride, chloride, nitrate, phosphate, and sulfate).

The concentration of carbon was determined from the quartz filters using the TOR® (DRI) Method. Two 0.64 cm^2 punches were taken from the quartz filter set on each stage of Andersen sampler and placed in the analyzer. Organic carbon (OC) was defined as all carbon that evolves from the sample without added oxygen when heated up to 550°C. Two additional temperature steps of 700°C and 800°C are made. Elemental carbon (EC) was defined as all carbon that evolves from the sample when heated up to 800°C in 2% oxygen in 98% helium atmosphere after the OC was removed. This TOR® method is a well-accepted technique in which the sample is progressively pyrolyzed with continuous detection of evolved carbon. Chow *et al*. (1993) gave a full detail of TOR® method.

2.3 Single Particle Analysis

The ultra trace elements in individual submicron particles (D_p, 0.65 μm) were identified by the X-ray microprobe system equipped at the Super Photon ring 8 GeV (SPring-8), BL-39XU. This X-ray microprobe system is composed of a sample scanning system, the KB mirror system (IRELEC co.) and a pinhole scanning system. To detect XRF from the sample present system is equipped with the conventional Si (Li) detector (Horiba, Ltd.) and a SDD (silicon drift detector) (Horiba, Ltd.) (Hayakawa *et al*., 2001). Through this micro-analytical technique based on the X-ray fluorescence (XRF) method, multiple elements were suc-

cessfully analyzed with femtogram level sensitivity.

A sample was placed on the XY scanning stage in a vacuum chamber, and the sample areas (500-1000 μm^2 each time) were selected randomly and scanned by the microbeam. The takeoff angle of 10° was used for the measurement of X-ray fluorescence. The intensity of the incident X-rays was monitored by an ionization chamber. The XRF elemental image of aerosol particles can be obtained via the scanning processes. The point analysis for individual particles was then carried out. The fluorescence X-rays were recorded with a Si (Li) detector placed in the electron orbit plane of the storage ring. The detector was mounted at 90° to the incident X-rays to minimize the background caused by the scattering. More details about analytical procedures and experimental setups used for XRF microprobe analysis were described elsewhere (Hayakawa *et al*., 2001). By means of this XRF analytical technique, a total of 400 particles collected in two different field campaigns were analyzed.

3. RESULTS AND DISCUSSION

3. 1 Simulated Trajectory of Particle Position during Wintertime Field Campaign

It is critical to estimate the impact of long-range transport of air pollutants from China on the chemical properties of particles collected at our sampling site. Hence, in the present study, in order to track particle movement during our sampling period, the time resolved (from Dec. 16 to Dec. 17, 2003) particle positions was simulated by the National Oceanic Atmospheric Administration (NOAA) HYSPLIT (HYbrid Single-

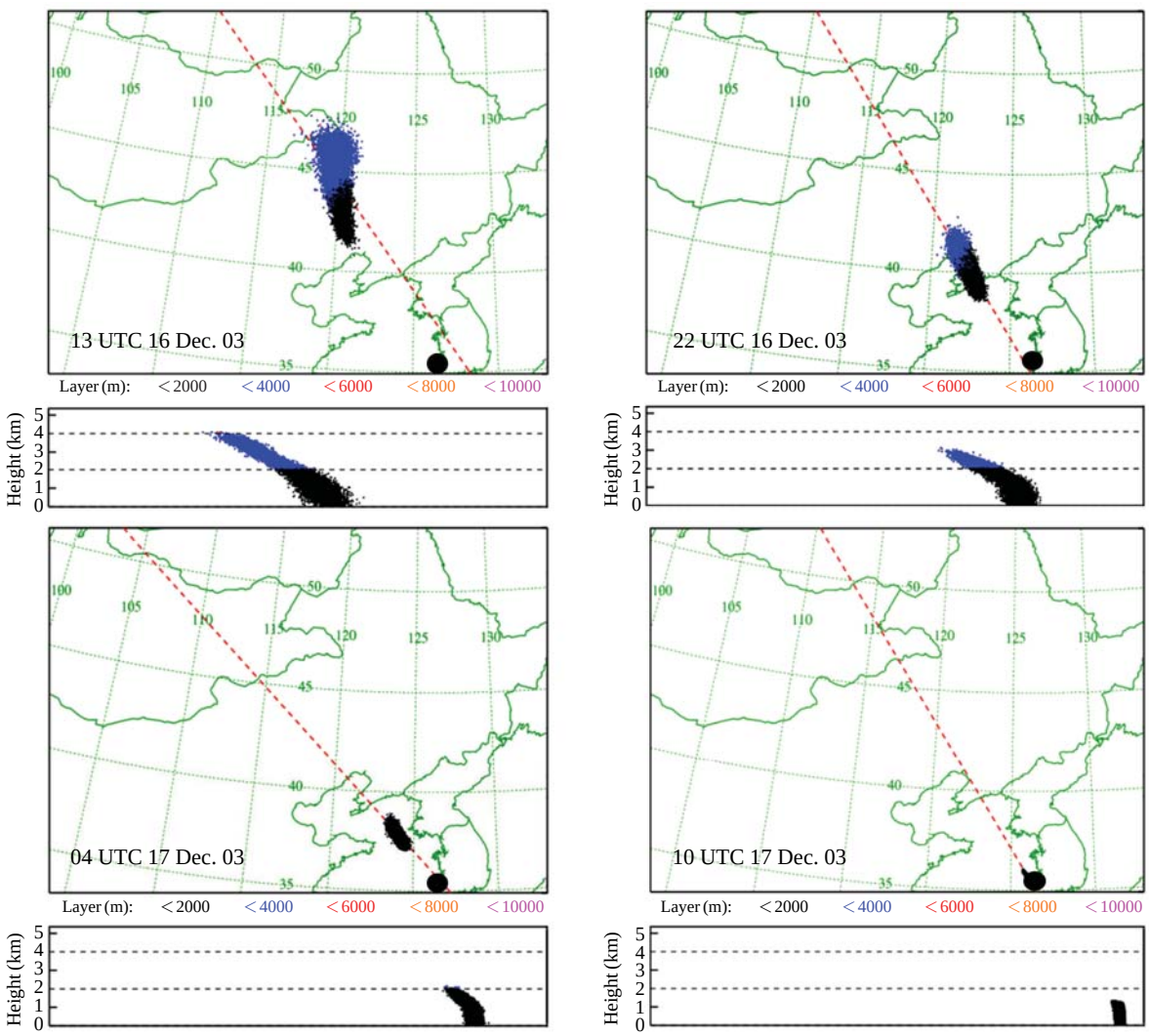

Fig. 1. Trajectory of particle position and cross-sections simulated by NOAA from Dec. 16 to Dec. 17, 2003.

Particle Lagrangian Integrated Trajectory) dispersion model. The starting location of trajectory of particles distribution was the sampling site (35.37°N; 126.27°E, the filled circle in Fig. 1) of Byunsan Peninsula. The cross-sectional distribution of particles depending on height was also shown at the bottom of each trajectory.

This trajectory is the time integration of the position of air as it is transported by the wind. The parcel's passive transport by the wind is computed from the average of the three-dimensional velocity vectors at the particle's initial-position and its first-guess position. The velocity vectors are interpolated in both space and time (Rolph, 2003). A detailed model description of HYSPLIT was given by Rolph (2003).

The results of simulated particle position indicate that the particles distributed in the northeastern of China bounded for the southwest part of the Korean Peninsula. Thus it suggests that the chemical characteristics of particles collected on the Byunsan Peninsula of Korea were directly affected by the particles emitted from China.

The strong winter monsoon in East Asia is characterized by an enhanced upper-level jet stream (Jhun and Lee, 2004). Kim (2000) studied the long-range transport of air pollutants in northeast Asia with isentropic trajectories. According to Kim's study (Kim, 2000), the counter of back trajectories from northwest and north in December accounted for 53% and 41% of total counters, respectively. This characteristic winter monsoon in East Asia not only results in the difference of the circulation in winter, but also affects the long-range transport of air pollutants.

3.2 Properties of Size-resolved Bulk PM

3.2.1 Source Fractionation of Size-classified PM

In order to access the source fraction of each size PM, the chemical composition of size-classified PM was fractionated into five components (i.e., EC, organic materials (OM), inorganic secondary pollutants (ISP), crustal matter (CM), and sea-salts (SS)). The amount of OM was determined by multiplying the concentration of OC by 1.4 (Countess *et al*., 1980). ISP was calculated by sum of the concentrations of NH_4^+, NO_3^-, and nss-SO_4^{2-}. SS was estimated by 3.27 [Na^+] (Ohta and Okita, 1990). CM concentration was constructed by the following equation, which takes into account the occupation ratio of Ca in crust and the ratio of water soluble Ca to total Ca (Ma *et al*., 2004; Hassett and Banwart, 1992): [CM]=32.79 [ionic Ca] [total Ca/soluble Ca]. The concentration variation of 5-source of size-classified PM is illustrated in Fig. 2. Detailed composition fraction of ISP is also shown at the upper of Fig. 2. The sum concentration of 5-source displays

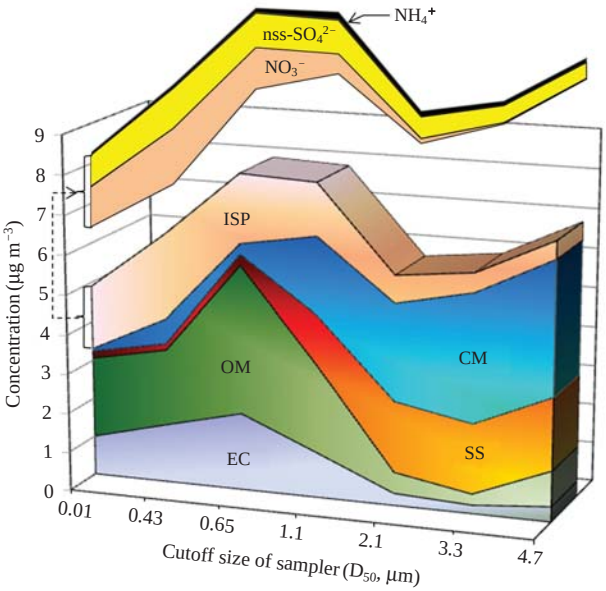

Fig. 2. Components (elemental carbon (EC), organic materials (OM), inorganic secondary pollutants (ISP), crustal matter (CM), sea-salts (SS)) distribution of size-resolved particles.

the bimodal with major peak in fine (D_p, 0.65 μm) fraction and minor peak in coarse (D_p, 4.7 μm) fraction. According to our expectation, ISP (mainly occupied by nss-SO_4^{2-} and NO_3^-), OM, and EC are enriched in fine fraction ($D_p < 1.1$ μm). It seems reasonable to say that these fine fraction sources were formed by a gas-to-gas reaction in the atmosphere or by the combustion process of fossil fuel. While on the other hand, SS and CM are the major contributors at the larger sizes (D_p, 3.3 μm-4.7 μm).

A comparative discussion of SS and CM concentrations in our sampling site and rural coat area of Japan will help to understand the peculiarity of PM collected in this study. Ito (2003) reported that SS and CM concentrations were 0.49 μg m^{-3} and 0.57 μg m^{-3} respectively in $PM_{5.1\text{-}3.5}$ collected at Yasaka (35.37°N, 135.81°E) located in Tango peninsula of Kyoto Prefecture, Japan during April 1-5, 2001. Though in view of the fact that Yasaka is a background site (TSP concentration was 19.7 μg m^{-3}) (Ito, 2003), CM (3.25 μg m^{-3}) and SS (1.78 μg m^{-3}) in $PM_{4.7\text{-}3.3}$ collected in our sampling site are overwhelmingly high. This result was partially caused by the Saemangum dam (located at 4 km northwest of Byunsan Beach) project. Because the Saemangum dam construction dramatically gave rise to bubble-blasting by activated waves and coming in and out of heavy duty vehicles and heavy equipment.

Fig. 3 shows the inter components correlation matrix among EC, OM, ISP, CM, and SS in size-resolved

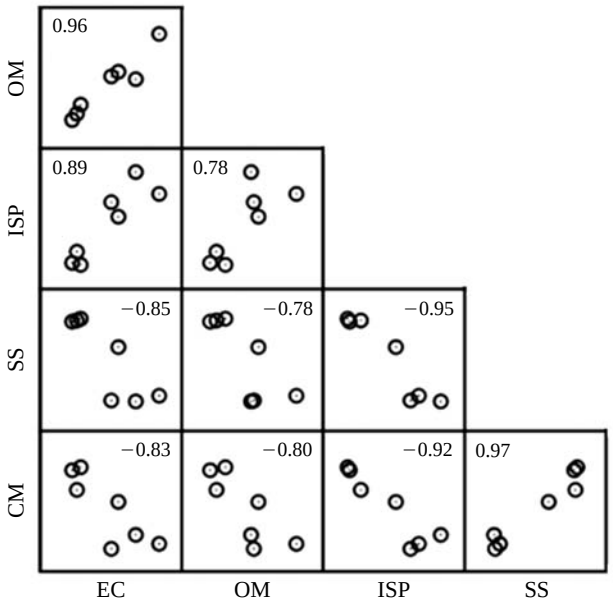

Fig. 3. The inter components (EC, OM, ISP, CM, and SS in size-resolved particles) correlation matrix. The numbers in plots mean Pearson's correlation coefficiency.

particles. This squared multiple correlation matrix was obtained from the inverted matrix of inter component correlations. As shown in Fig. 3, highly positive correlationships are found between 3 pairs (i.e., OM vs. EC, ISP vs. EC, and CM vs. SS). Their Pearson's correlation coefficiencies are 0.96, 0.89, and 0.97, respectively.

Although OC contains a significant amount of non-combustion which is referred to the biogenic primary OC or regional OC background, the scatter plot of OM and EC in size segregated PM shows that OM mainly derived from combustion process with EC. As a matter of course, as the common ISP, ammonium sulphate and ammonium nitrate formed from ammonia, sulphuric acid, and nitric acid have a good interrelation with EC. As mentioned earlier, human activities, that is, the Saemangum Project which was actively progressing during our field measurement might be promotive of blowing soil particles off the ground. Added to this, the inflow of sea salt particles into the atmosphere might be activated by dropping rocks to sea for land reclamation made.

3.2.2 Carbonaceous Components in Size-classified Fine PM

Concentrations of EC and OC as well as the ratio of OC to EC in size-fractionated fine PM collected in two different seasons are listed in Table 1. Both EC and OC concentrations fluctuate depending on the particle size during two sampling periods. The maximum levels of EC and OC were ranked in $PM_{1.1\text{-}0.65}$ in wintertime. Similar size-distribution of OC concentration was found in springtime. However, the maximum concentration of EC shifts to in a range of 0.43-0.65 μm.

Table 1. Carbonaceous components in size-fractionated fine particles.

Particle fraction	Concentration (μg m^{-3})			OC/EC
	OC	EC	TC	
Winter				
$PM_{2.1\text{-}1.2}$	1.60	1.15	2.74	1.39
$PM_{1.1\text{-}0.65}$	2.69	1.97	4.66	1.37
$PM_{0.65\text{-}0.43}$	1.63	1.65	3.28	0.99
$PM_{0.43\text{-}0.01}$	1.46	1.00	2.47	1.46
Spring				
$PM_{2.1\text{-}1.2}$	1.04	0.69	1.73	1.49
$PM_{1.1\text{-}0.65}$	1.98	1.20	3.19	1.65
$PM_{0.65\text{-}0.43}$	1.38	1.50	2.88	0.92
$PM_{0.43\text{-}0.01}$	1.39	1.04	2.43	1.34
Winter/Sping				
$PM_{2.1\text{-}1.2}$	1.54	1.65	1.58	–
$PM_{1.1\text{-}0.65}$	1.36	1.64	1.46	–
$PM_{0.65\text{-}0.43}$	1.18	1.10	1.14	–
$PM_{0.43\text{-}0.01}$	1.05	0.96	1.02	–

Salcedo *et al*. (2005) carried out the particle size distribution of carbon in the atmosphere of Mexico City during wintertime and reported that the major peak of EC was formed at the 0.18-0.32 μm size range. The particles showing the maximum EC concentration in this study were larger in size compared to those collected in Mexico.

The composition and structure of freshly emitted soot depend to a large extent on the character of the combustion (Moosmüller *et al*., 2009). In the atmosphere, EC is present in the form of chain aggregates of small soot globules. It is, therefore, suggested that the soot aggregates in our sampling site uptook other inorganic or organic compounds in the proximity of emission region during aging processes and/or long-range transport.

The concentrations of EC in $PM_{1.1\text{-}0.01}$ in winter and spring times were 4.62 μg m^{-3} and 3.74 μg m^{-3}, respectively. Meanwhile, the daily Gosan (the western tip of Jeju Island) mass concentrations of EC in $PM_{1.0}$ from March 30 and May 2, 2001 varied from 0.15 μg m^{-3} to 1.55 μg m^{-3} (Chuang *et al*., 2003). The average winter/spring ratio of EC concentration (1.23) suggests that EC concentration in wintertime is high in comparison to that in springtime. This high wintertime EC concentration in Byunsan region was also probably caused by both the mobilized equipments for the Saemangum Project and long-range transport.

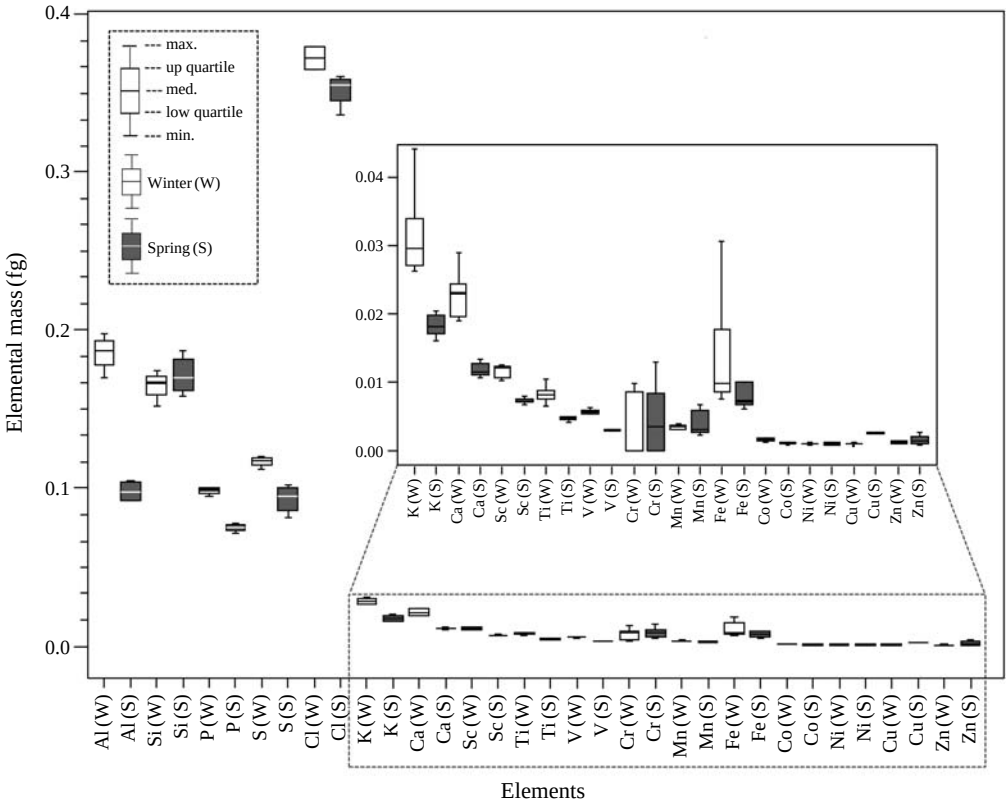

Fig. 4. Box plots of each elemental mass of submicron particles (D_p, 0.65 μm). Elemental mass was calculated by X-ray microprobe system equipped at SPring-8, BL-39XU. Total particle number is 150.

Although it is a real hardship to accurately measure the particulate OC concentration because of both its volatilization (i.e., negative artifact) and adsorption of gas-phase organics onto the filter (i.e., positive artifact) during and/or after sampling, the ratio of OC to EC listed in the last column of Table 1 is often used as a valuable tool for the identification of the secondary OC (Turpin *et al*., 2000; Turpin and Huntziker, 1995).

The wintertime OC/EC ratio is varied in a range between 0.99 and 1.39 with average level of 1.3 in $PM_{1.1\text{-}0.01}$ in wintertime. The OC/EC ratio measured in this study is comparable to those observed at other urban sites, i.e., 6.2 in $PM_{1.5}$ at San Pietro, Italy in falltime (Zappoli *et al*., 1999), 16.9 in $PM_{2.5}$ at K-puszta, Hungary in summertime (Molnár *et al*., 1999). At a rural location in northern Michigan, US in wintertime, OC/EC ratio was 3.3 (Cadle and Dasch, 1988).

In general, a seasonal peak in the ratio of OC to EC in fine particles is observed during the summer photochemical season, reflecting an increased formation of secondary organic carbon. From this point of view, relatively low OC/EC ratio obtained in the present study compared to those reported at other urban and rural sites might be explained by the fact that our wintertime measurement period was not favorable meteorological conditions for the gas-particle conversion of gaseous hydrocarbon precursors as a result of photochemical activity. Furthermore, the low OC/EC ratio in Byunsan Peninsula can be attributed to the high EC concentration.

3.3 Elemental Properties of Individual Submicron PM

3.3.1 Elemental Mass

Elemental mass of submicron particles (D_p, 0.65 μm) individually determined by the X-ray microprobe system equipped at SPring-8, BL-39XU is summarized as both the empty box with (W; winter) and the filled box with (S; spring) in Fig. 4. According to Fig. 4, every element is classified into two groups, i.e., the major elements (Cl, Al, Si, S, and P) showing relatively high mass levels and the minor trace elements. Among the major elements, Cl shows preponderantly high mass compared with other elements. In view of the particle size, it is difficult to accept that Al, Si, and P were originated soil.

Mamane *et al.* (1986) reported that fly ash from coal consists primarily of aluminosilicates with a surface layer of sulfates. More detailed measurements of chemical composition of submicron particles emitted from coal burning were performed by Smith *et al.* (1979) and Querol *et al.* (1995). They reported that the largest elemental contributions were from Al, Si, and O (typically 12%, 22%, and 42%, respectively), with Fe, P, S, K, Ca, N, and Mg contributing up to 11%.

As one of local emission sources in the Byunsan Peninsula during our field campaign, the Gunsan thermal power generation station, which was operated from 1968 to 2007, was located in the northeast site about 50 km far away from our ground based particle sampling site. However, this local point source can be ruled out from the possible factor that influences the elemental properties of submicron particles because of the simulated trajectory of particle position discussed earlier.

Based on the overall consideration (i.e., particle size, the chemical composition of submicron particles generated from coal burning mentioned above, the fact the Chinese people rely heavily on coal as their main source of energy consumption, and the wintertime meteorological condition in East Asia), the elemental properties of individual submicron particles were strongly associated with long-range transport. Moreover, it turned out that the Taean thermal power generation station (36.17°N; 126.13°E) that is being operated with the imported coal from China emits fine fraction fly ash containing a large amount of Cl (Ma *et al.*, 2010).

About the Cl enrichment of individual submicron particles, details are discussed at the next part of this manuscript.

3. 3. 2 Clustering of Elements

Cluster analysis that is commonly used in environmental studies to classify the variable data taken at receptors was completed using SPSS software (version 16) for the thorough estimating of Cl source. The elemental masses of individual submicron particles (D_p, 0.65 μm) were subjected to cluster analysis. The result of cluster analysis is shown in Fig. 5 as dendrograms which summarize the process of clustering.

Both Cluster-2 (Al, Si, S, and P) and Cluster-3 (K, Ca, and Fe) are presumably representative of the chemical compositions of submicron particles emitted from coal burning. These two clusters are in agreement with the major (Al, Si, and O) and minor (Fe, P, S, K, Ca, N, and Mg) coal burning compositions suggested by Querol *et al.* (1995) and Smith *et al.* (1979).

The scatter plots (the inner part of Fig. 5) of elemental (except for Cl) masses between the individual particles in the present study and the individual granules of coal-fired fly ash (Ma *et al.*, 2010) reveals a good relationship (R^2=0.84). Meanwhile, the R-square value calculated from total elements, including Cl, is 0.56. In other words, the atmospheric environment of the Byunsan Peninsula is likely to be influenced significantly by long-range transport.

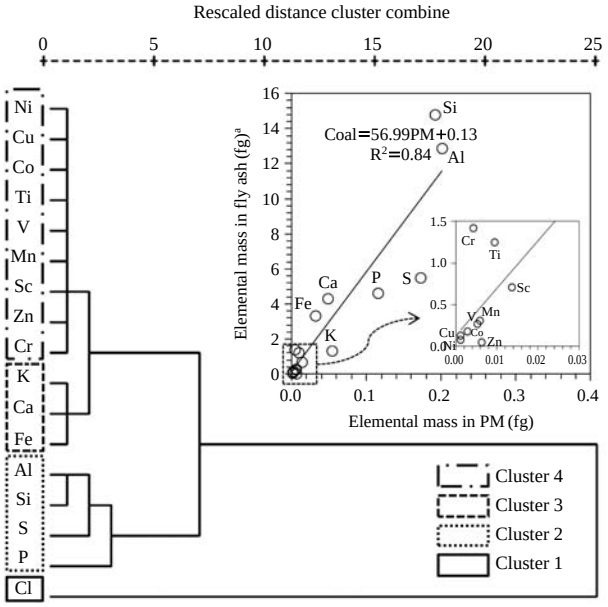

Fig. 5. The dendrogram of cluster analysis for the elements determined single particle (D_p, 0.65 μm) analysis by the Spring-8 XRF system (outer). Scatter plots of elemental masses between the individual particles (D_p, 0.65 μm) in the present study and the individual granules of coal-fired fly ash (a, Ma *et al.*, 2010) (inner).

Meanwhile, it is speculated that Cl has different property of source profile from those of others because it is classified as an independent cluster. It is essential to definitely categorize the Cl source at the Byunsan Peninsula.

Although it is generally understood that sea-salt belongs to coarse fraction, previous field measurements showed the presence of a large fraction of sea salt particles in the sub-micrometer aerosol (Nilsson *et al.*, 2001; Murphy *et al.*, 1998). In addition, a global model study by Pierce and Adams (2006) used new sea salt flux between 70 nm and 20 μm dry diameter. Clarke *et al.* (2006) found that over the Southern Ocean ultrafine sea salt can increase CCN concentrations by more than 50%.

As previously point out, an enormous amount of soil and stone for the land reclamation of Saemangeum was dumped into sea. In this process, it is logical to assume that sea salt emissions increased largely. Thus, although various polluters in both receptor area (e.g.,

automobiles and small scale farming incinerations) and China's domestic sources (e.g., coal burning for daily cooking and crop drying and coal-fired power station) can also be considered as the sources of ambient Cl at our sampling site, it seems reasonable to say that the high elemental mass loading of Cl in Fig. 4 and its solo categorizing in Fig. 5 were mainly due to the Saemangeum seawall project.

Many trace elements classed as Cluster-4 will be discussed in the next chapter.

3.3.3 Trace Elements

Fig. 6 shows the example of XRF elemental spectra for two randomly selected individual particles (the dotted and bold lines in the figure) from the irradiated particles by microbeam. These XRF spectra can be drawn by counting XRF counts of each element during the point analysis. Here, we lay emphasis on the interpretation of the minor trace elements distinctly detected in individual particles. Several minor trace elements like Cr (in particle described by the dotted line), Mn (in both particles), Zn (in both particles), and As and/or Pb (in both particles) show high XRF count. Elsewhere, the magnified XRF spectra at the bottom of Fig. 6 also show the meaningful peaks of Ga and Se that were presumably originated from coal burning.

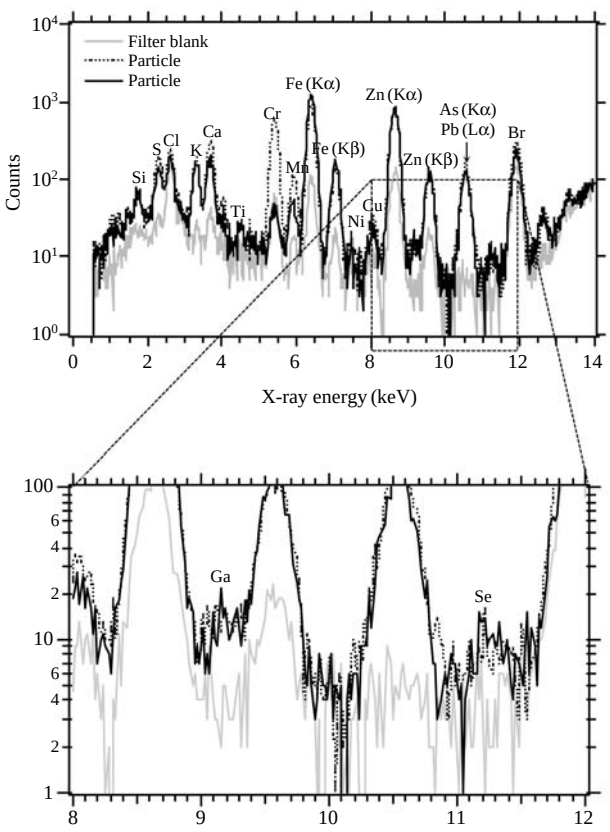

Fig. 6. An example of XRF elemental spectra for two randomly selected individual particles from the irradiated particles by microbeam.

Brigden *et al*. (2002) reported that fly ashes from coal combustion typically contained many highly toxic elements. These include manganese, nickel, zinc, arsenic, cobalt, lead, mercury, and certain forms of chromium. A number of these elements have also the potential to bioaccumulation (Liu *et al*., 2002).

4. CONCLUSIONS

The goal of our field study was the measurement of wintertime PM and related compositions to investigate the large amount of pollutant inflow from both the Saemangeum Project and long-range transport. As the result of our field measurement, the collaborative situation among the mobilization of equipments (e.g., numerous heavy dump trucks and dredging equipments), an extensive reclamation construction, and the long-range transport by winter monsoon leads to the increase in atmospheric pollutants, especially, crustal matter, sea-salts, elemental carbon, and coal-fire origin particulate matters in the Byunsan Peninsula. It is considered that the results of this study will be valuable for a better understanding of the influx of pollutants from the biggest artificial land reclamation project and China continent.

ACKNOWLEDGEMENT

The authors gratefully acknowledge all the members of SPring-8, BL-39XU, Prof. S. Tohno at Graduate School of Energy Science, Kyoto University, and Prof. K. Sera at Cyclotron Research Center, Iwate Medical University for their cooperation with micro-XRF analysis and PIXE analysis. The authors also thank Ph.D. R. Cao, Tokyo Dylec Co., for carbon analysis. The HYSPLIT aerosol dispersion model (http://www.arl.noaa.gov/ready.html) developed by the National Oceanic Atmospheric Administration (NOAA) was very helpful to data interpretation.

REFERENCES

Brigden, K., Santillo, D., Stringer, R. (2002) Hazardous emissions from Thai coal-fired power plants: Toxic and potentially toxic elements in fly ashes collected from the Mae Moh and Thai Petrochemical Industry coal-fired power plants in Thailand, Technical Note of Greenpeace Research Laboratories, University of Exeter, UK, pp. 1-20.

Cadle, S.H., Dasch, J.M. (1988) Wintertime concentrations and sink of atmospheric particulate carbon at a rural location in northern Michigan. Atmospheric Environment 22, 1373-1381.

Chow, J.C., Watson, J.G., Pritchett, L.C., Pierson, W.R., Frazier, C.A., Purcell, R.G. (1993) The DRI thermal/optical reflectance carbon analysis system: description, evaluation and applications in US air quality studies. Atmospheric Environmen 27A, 1185-1201.

Chuang, P.Y., Duvall, R.M., Bae, M.S., Jefferson, A., Schauer, J.J., Yang, H., Yu, J.Z., Kim, J. (2003) Observations of elemental carbon and absorption during ACE-Asia and implications for aerosol radiative properties and climate forcing. Journal of Geophysical Research 108, D23, 8634, doi:10.1029/2002JD003254.

Clarke, A., Owens, S., Zhou, J. (2006) An ultrafine sea-salt flux from breaking waves: Implications for cloud condensation nuclei in the remote marine atmosphere. Journal of Geophysical Research 111, D06202, doi: 10.1019/2005JD006565.

Gulyas, H., Gercken, G. (1988) Cytotoxicity to alveolar macrophages of airborne particles and waste incinerator fly-ash fractions. Environmental Pollution 51, 1-18.

Hassett, J.J., Banwart, W.L. (1992) Soils and their environment. Prentice-Hall Inc. Englewood Cliffs, New Jersey, NJ.07632.

Hayakawa, S., Ikuta, N., Suzuki, M., Wakatsuki, M., Hirokawa, T. (2001) Generation of an X-ray microbeam for spectromicroscopy at SPring-8 BL39XU. Journal of Synchrotron Radiation 8, 328-330.

Ito, K. (2003) Size-resolved optical and chemical properties of atmospheric aerosols observed in Tango Peninsula during ACE-Asia. Master degree thesis of Graduate School of Energy Science, Kyoto University (in Japanese).

Jajuminbo (2010) The Saemangeum seawall project, http://jajuminbo.net/sub_read. html?uid=6083&section=sc18.

Jhun, J.G., Lee, E.J. (2004) A new East Asian winter monsoon index and associated characteristics of the winter monsoon. Journal of Climate 17, 711-726.

Kim, S.Y. (2000) A study of long-range transport of air pollutants in northeast Asia with isentropic trajectories. Master degree thesis of Seoul National University (in Korean).

Liu, J., Zheng, B., Aposhian, V., Zhou, Y., Chen, M.L., Zhang, A., Waalkes, M.P. (2002) Chronic arsenic poisoning from burning high-arsenic-containing coal in Guizhou, China. Search Results. Environmental Health Perspectives 110, 119-122.

Ma, C.J., Kim, J.H., Kim, K.H., Tohno, S., Kasahara, M. (2010) Specification of chemical properties of feed coal and bottom ash collected at a coal-fired power plant. Asian Journal of Atmospheric Environment 4(2), 80-88.

Ma, C.J., Oki, Y., Tohno, S., Kasahara, M. (2004) Assessment of wintertime atmospheric pollutants in an urban area of Kansai, Japan. Atmospheric Environment 38, 2939-2949.

Mamane, Y., Miller, J.L., Dzubay, T.G. (1986) Characterization of individual fly-ash particles emitted from coal- and oil-fired power plants. Atmospheric Environment 20, 2125-2135.

McDonnell, W.F., Nishino-Ishikawa, N., Petersen, F.F., Chen, L.H., Abbey, D.E. (2000) Relationships of mortality with the fine and coarse fractions of long-term ambient SPM concentrations in nonsmokers. Journal of Exposure Analysis and Environmental Epidemiology 10, 427-436.

Molná, Á., Mészáros, E., Hansson, H.C., Karlsson, H., Gelencsér, A., Kiss, Gy., Krivácsy, Z. (1999) The imortance of organic and elemental carbon in the fine atmospheric aerosol particles. Atmospheric Environment 33, 2745-2750.

Moosmüller, H., Chakrabarty, R.K., Arnott, W.P. (2009) Aerosol light absorption and its measurement: a review. Journal of Quantitative Spectroscopy & Radiative Transfer 110, 844-878.

Murphy, D.M., Anderson, J.R., Quinn, P.K., McInnes, L.M., Brechtelk, F.J., Kreidenweisk, S.M., Middlebrook, A.M., Pósfai, M., Thomson, D.S., Buseck, P.R. (1998) Influence of sea-salt on aerosol radiative properties in the Southern Ocean marine boundary layer. Nature 392, 62-65.

Nilsson, E.D., Rannik, Ü., Swietlicki, E., Leck, C., Aalto, P.P., Zhou, J., Norman, M. (2001) Turbulent aerosol fluxes over the Arctic Ocean 2. Wind-driven sources from the sea. Journal of Geophysical Research 106, 32 111-32 124.

Ohta, S., Okita, T. (1990) A chemical characterization of atmospheric aerosols in Sapporo. Atmospheric Environment 24A, 815-822.

Pierce, J., Adams, P. (2006) Global evaluation of CCN formation by direct emission of sea salt and growth of ultrafine sea salt. Journal of Geophysical Research 111, D06203, doi:10.1029/2005JD006186.

Pope, C.A., Hill, R.W., Villegas, G.M. (1999) Particulate air pollution and daily mortality on Utah's Wasatch Front. Environmental Health Perspectives 107, 567-573.

Querol, X., Fernadez-Turiel, J.L., Lopez-Soler, A. (1995) Trace elements in coal and their behavior during combustion in a large power station. Fuel 74, 331-343.

Rolph, G.D. (2003) Real-time Environmental Applications and Display system (READY) Website (http://www.arl.noaa.gov/ready/hysplit4.html). NOAA Air Resources Laboratory, Silver Spring, MD.

Salcedo, D., Dzepina, K., Onasch, T.B., Canagaratna, M.R., Jayne, J.T., Worsnop, D.R., Gaffney, J.S., Marley, N.A., Johnson, K.S., Zuberi, B., Molina, L.T., Molina, M.J., Shutthanandan, V., Xie, Y., Jimenez, J.L. (2005) Characterization of ambient aerosols in Mexico City during the CMA-2003 campaign with Aerosol Mass Spectrometry-Part II: overview of the results at the CENICA supersite and comparison to previous studies. Atmospheric Chemistry and Physics Discussions 5, 4183-4221.

Smith, R.D., Campbell, J.A., Nielson, K.K. (1979) Characterization and formation of submicron particles in coal-fired plants. Atmospheric Environment 13, 607-617.

Turpin, B.J., Huntziker, J.J. (1995) Identification of secondary organic aerosol episodes and quantitation of primary and second organic aerosol concentration during SCAQS. Atmospheric Environment 29, 3527-3544.

Turpin, B.J., Sazena, P., Andrews, E. (2000) Measuring and simulating particulate organics in the atmosphere: problems and prospects. Atmospheric Environment 34, 2983-3013.

Wang, Z., Ueda, H., Huang, M. (2000) A deflation module for use in modeling long-range transport of yellow sand over East Asia. Journal of Geophysical Research 105, 26947-26960.

Zappoli, S., Andracchio, A., Fuzzi, S., Facchini, M., Gelencser, A. (1999) Inorganic, organic and macromolecular components of fine aerosol in different areas of Europe in relation to their water solubility. Atmospheric Environment 33, 2733-2743.

(Received 6 April 2012, revised 13 September 2012, accepted 13 September 2012)